Flow-Induced Concentration Nonuniformity and Shear Banding in Entangled Polymer Solutions

Michael C. Burroughs,[1] Yuanyi Zhang,[1] Abhishek M. Shetty,[2] Christopher M. Bates,[1,3] L. Gary Leal,[1,*] and Matthew E. Helgeson[1,†]

[1]Department of Chemical Engineering, University of California, Santa Barbara, Santa Barbara, California 93106, USA
[2]Anton Paar USA, Inc., Ashland, Virginia 23005, USA
[3]Department of Materials, University of California, Santa Barbara, Santa Barbara, California 93106, USA

(Received 9 October 2020; revised 14 April 2021; accepted 21 April 2021; published 20 May 2021)

Recent models have predicted entangled polymer solutions could shear band due to unstable flow-induced demixing. This work provides the first experimental probe of the *in situ* concentration profile of entangled polymer solutions under shear. At shear rates above a critical value, we show that the concentration and velocity profiles can develop bands, in quantitative agreement with steady-state model predictions. These findings highlight the critical importance of flow-concentration coupling in entangled polymer solutions.

DOI: 10.1103/PhysRevLett.126.207801

Traditionally, it is assumed that the flow of entangled polymeric fluids in shear-based rheometric devices is homogeneous across the polymeric fluid [1,2]; however, important departures from homogeneous flow can sometimes occur [3]. For example, the flow can become shear banded with two or more regions of locally distinct shear rates under an applied shear flow [4,5]. Such nonhomogeneous flows have been observed in numerous complex fluids including wormlike micelles [6–11], telechelic polymers [12], and soft colloidal glasses [13,14], but the existence of shear banded flows in entangled polymer solutions has remained elusive [15–20] and has sparked immense controversy in recent years [21–24]. If entangled polymeric liquids do indeed shear band, then prior interpretations of the nonlinear flow behavior, and models for entangled polymer rheology more generally, will need to be reconsidered to account for the large spatial inhomogeneities present in the flow.

Commonly, shear banding has been explained as the result of a constitutive instability [5,25], where an underlying nonmonotonic dependence of shear stress on the shear rate leads to a range of applied shear rates where uniform shear flow is unstable. With reference to entangled polymers, decades of experimental measurements [26–28] and resulting modifications to constitutive models [29–33] have led most to believe that the constitutive relationship is monotonic, seeming to preclude the possibility of shear banding for compositionally homogeneous polymeric liquids. Despite this perceived consensus, evidence of shear banded velocity profiles in polymer solutions has been reported [15–18,26,34,35]. Recently, conflicting conclusions regarding the existence of shear banding in entangled polymers were reported [15,23], as determined from particle tracking velocimetry (PTV) measurements, even though the entanglements per molecule (Z) and dimensionless applied shear rates

$$Wi_{\mathrm{app}} = \tau_d \dot{\gamma} \tag{1}$$

were held fixed. Here, τ_d represents the longest relaxation time and $\dot{\gamma}$ is the nominal shear rate. A notable distinction in these two studies is the difference in polymer-solvent system used; however, the possible role of solution thermodynamics on the resulting flow was not addressed. Instead, inconsistencies in the measured flow profiles were argued to arise from several artifacts including edge fracture [21,36], secondary flows [21], unsteady flow [16], and even issues with how data were analyzed [24]. Clearly, the existence of shear banding in entangled polymer solutions remains an unresolved issue, and to reach consensus there is a strong need to support any experimental results with a fundamental theoretical description of the underlying physics.

Constitutive instability is not the only possible explanation for why steady shear banded flows might develop. Models that incorporate an explicit coupling between the polymer concentration and the stress, so-called two-fluid models, predict regions of parameter space where a homogeneous, linear shear flow is unstable to infinitesimal perturbations in polymer concentration [37–43]. This instability is predicted to result in a shear-induced demixing of polymer and solvent to form gradients in polymer concentration on macroscopic length scales [44], which coincide with banded velocity profiles, even with monotonic constitutive behavior [37–39]. The propensity for shear-induced demixing in entangled polymer solutions is shown by the theory to depend on the flow-concentration coupling parameter E,

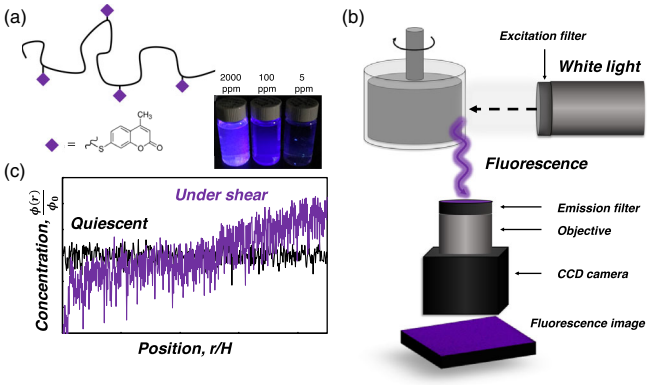

FIG. 1. (a) Cartoon of PBD tagged with coumarin fluorophore (PBDC) and the resulting fluorescence across a concentration series of PBDC (vials); (b) rheofluorescence setup with 350 nm incident light and emission wavelengths filtered to 415 nm; (c) representative data for quiescent fluorescence versus fluorescence measured under shear.

$$E = \frac{G(\phi)}{\chi^{-1}\phi^2}, \tag{2}$$

with $G(\phi)$ being the concentration-dependent shear modulus, χ^{-1} the osmotic susceptibility, and ϕ the polymer concentration [37–39]. Thus, the polymer-solvent system specific value of E provides one possible explanation for why banding is observed in some solutions but not others (despite comparable Z and Wi_{app}).

In the two-fluid model, polymer migration arises via an imbalance between the elastic, osmotic, and drag forces acting on the polymers. This migration can amplify thermal fluctuations in concentration, known as shear-enhanced concentration fluctuations (SECF), and also lead to macroscopically inhomogeneous flow starting from a shear-induced demixing instability at higher shear rates. The microscale nonuniformities in polymer concentration due to SECF [45,46] have been confirmed by indirect measurements, such as *in situ* small angle scattering, in entangled polymer solutions under shear [45,47–50]. However, no prior experiments have demonstrated that gradients in concentration indeed form on macroscopic length scales in entangled polymer solutions.

In this Letter, we report measurements of both the velocity and concentration profiles in entangled polybutadiene (PBD) in dioctyl phthalate (DOP) solutions under a range of applied shear rates. The data demonstrate that the predicted shear-induced demixing instability does occur in entangled polymer solutions, and results in gradients of both concentration and shear rate on macroscopic length scales. The concentration measurements rely on a novel rheofluorescence methodology to visualize and estimate macroscopic changes in polymer concentration (Fig. 1).

Entangled polymer solutions with $Z = 38$ (10 wt %) were prepared by dissolving low-dispersity 1,4-Polybutadiene [PBD(1 M), $M_w = 9.6 \times 10^5$ g/mol, Đ = 1.08, Polymer Standards Services] in dioctyl phthalate (DOP, Sigma-Aldrich). All measurements were performed at $T = 50\,^{\circ}\mathrm{C}$. For this temperature, we approximate the PBD-DOP solution to exhibit behavior intermediate to theta and good solvent conditions. Approximately 10 μm glass tracer particles (TSI, Inc.) were suspended in the entangled solution (300 ppm) for rheo-PTV measurements. 2000 ppm of fluorescently tagged PBD (PBDC; synthesis details in Supplemental Material [51]) was added to the solution for rheofluorescence measurements.

Velocity profiles were measured by rheo-PTV using a custom optical setup fitted to a Paar Physica MCR 300 rheometer [52–54]. One important feature for this study is the startup mode, which goes from rest to steady rotation in 0.05 s. The diameter of the inner cylinder is 34 mm and the curvature ratio is 0.029. The aspect ratio is 2.125. Steady-state velocity profiles were determined by averaging the velocity profiles determined from individual image pairs over time after the measured shear stress reached a steady value.

Concentration profiles were determined using a new combined rheometry and *in situ* fluorescence imaging technique ("rheofluorescence") using an Anton Paar MCR 702 rheometer. The transparent Taylor-Couette cup and anodized aluminum bob were identical to those used in rheo-PTV measurements [52–54], however, the Anton Paar MCR 702 shear startup process takes 1 s. The fluorescence intensity of the PBD-DOP solution with trace PBDC was monitored during shear flow at different Wi_{app} ($\tau_d = 1.9$ s). A Xenon light source (ASB-XE-175, 250 W, Spectral Products) was filtered to the excitation wavelength of the fluorophore (350 nm) to irradiate the entangled polymer solution with trace PBDC. The fluorescence emission signal passes through a 415 nm bandpass filter before reaching the CCD detector. Relative changes in the local polymer concentration from the initial uniform state were determined by monitoring changes in the intensity of the fluorescence image relative to the background and normalized by the quiescent image given by

$$\frac{\phi(r,t,\dot{\gamma})}{\phi_o} \approx \frac{I(r,t,\dot{\gamma}) - I_{bg}}{I_o - I_{bg}}. \tag{3}$$

Here, $\phi(r)/\phi_o$ is the normalized polymer concentration, $I(r,t,\dot{\gamma})$ is the transient fluorescence intensity at a particular applied shear rate, I_{bg} is the background intensity without illumination, and I_o is the fluorescence intensity at rest.

An example of the measured steady-state velocity profiles of the entangled PBD(1 M)-DOP solution is shown in Fig. 2, together with two-fluid (Rolie-Poly, $R-P$) model [38] predictions for several values of E. The velocity profiles were collected after shearing for at least 50 τ_d and averaged over time using greater than 2000

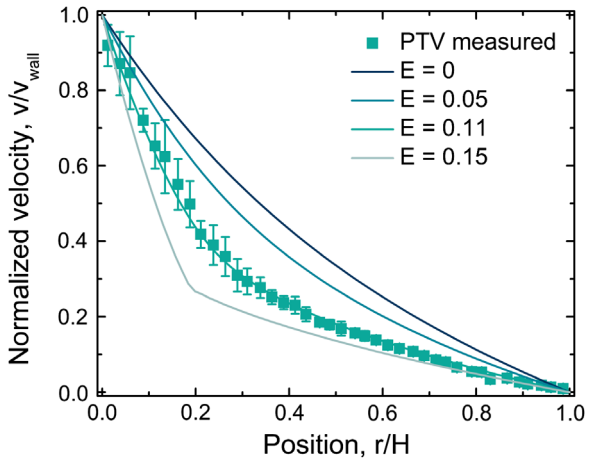

FIG. 2. Steady-state velocity profile of 10 wt % PBD(1 M)-DOP with $Z = 38$ at $Wi_{app} = 5$ with model fits for varying E. The position (r/H) is determined by normalizing the radial distance from the moving wall (r) by the fluid thickness (H).

data points. The small associated standard errors suggest that these data reflect the steady-state flow profiles. Although this timescale to steady state is significantly shorter than one might expect from either the stability analysis or previous numerical simulations of the two-fluid model in a linear shear flow [38], this is not surprising. First, while the previous analyses began from the homogeneous flow solution with uniform concentration, the experiments are implemented via an abrupt startup from rest as noted above. Second, the intrinsic curvature of the Couette device will also shorten the timescale [39]. Last, the magnitude of perturbations in concentration for experiments are likely larger than what was previously investigated theoretically.

The profile in Fig. 2 exhibits variations in the local shear rate that are much greater than would occur in a homogeneous fluid due to the combination of shear thinning and the intrinsic curvature of the Taylor-Couette flow cell. (calculations in Supplemental Material [51]). Furthermore, as shown in Fig. 2, the homogeneous $R-P$ model predictions ($E = 0$) also underpredict the measured variations in the local shear rate despite again accounting for the curvature of the Taylor-Couette flow cell and the shear thinning of the fluid.

In contrast, the two-fluid $R-P$ model [39] provides an excellent fit of the data for $E = 0.11$ (Fig. 2). $E = 0.11$ is a reasonable value for theta solutions where E is estimated to be $O(0.1)$ [55]. Although the velocity profile does not appear sharply banded, it is in fact a shear banded profile as shall be discussed shortly. We note that the theory predicts more sharply banded profiles than exhibited in Fig. 2 for entangled polymer systems with higher Z and larger values of E [37–39], as shown in the Supplemental Material [51].

The value of E is intrinsic to the polymer-solvent system, since $G(\phi)$ depends on the number of Kuhn monomers in an entanglement strand (N_e) and χ^{-1} is sensitive to the solvent quality. Thus, the value of $E = 0.11$, obtained by fitting data for one value of Wi_{app}, yields remarkable agreement between model predictions of the flow profiles and the measured velocimetry data across a wide range of Wi_{app} (Fig. 3).

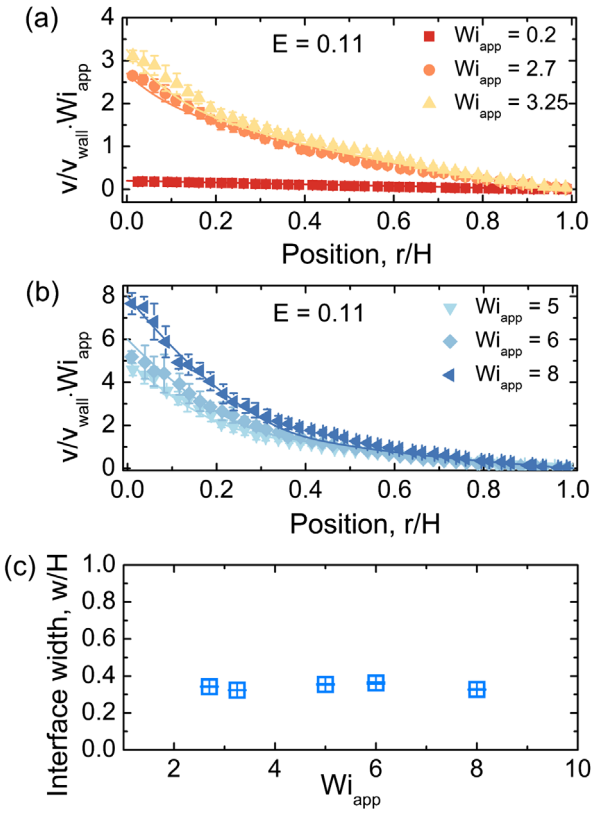

FIG. 3. (a),(b) Steady-state velocity profiles for varying Wi_{app} at $T = 50$ °C. Symbols correspond to experimentally measured values from rheo-PTV and solid lines are two-fluid model predictions for $E = 0.11$. (c) Interface widths of the flow profiles calculated using the method detailed in [53].

In spite of the fact that the velocity profiles show much more curvature than would be the case from the combination of the flow geometry-imposed curvature and shear thinning in a homogeneous fluid, one may still question whether the velocity profiles in Fig. 3 are truly "banded." To address this point, a previously proposed model-free experimental procedure for calculating the interface width between "bands" [53] of the velocity profiles is employed. It was shown in [53] that the width of the interface remains invariant to changes in the applied shear rate, for shear banded velocity profiles. This property is confirmed in Fig. 3(c), providing strong evidence that the experimental flow profiles are indeed shear banded. A more detailed investigation of this and related findings is left to ongoing investigations, including the sensitivity of the apparent interface width to changes in fluid properties (such as E and Z).

Turning now to the rheofluorescence measurements during shear, we show transient concentration profiles in

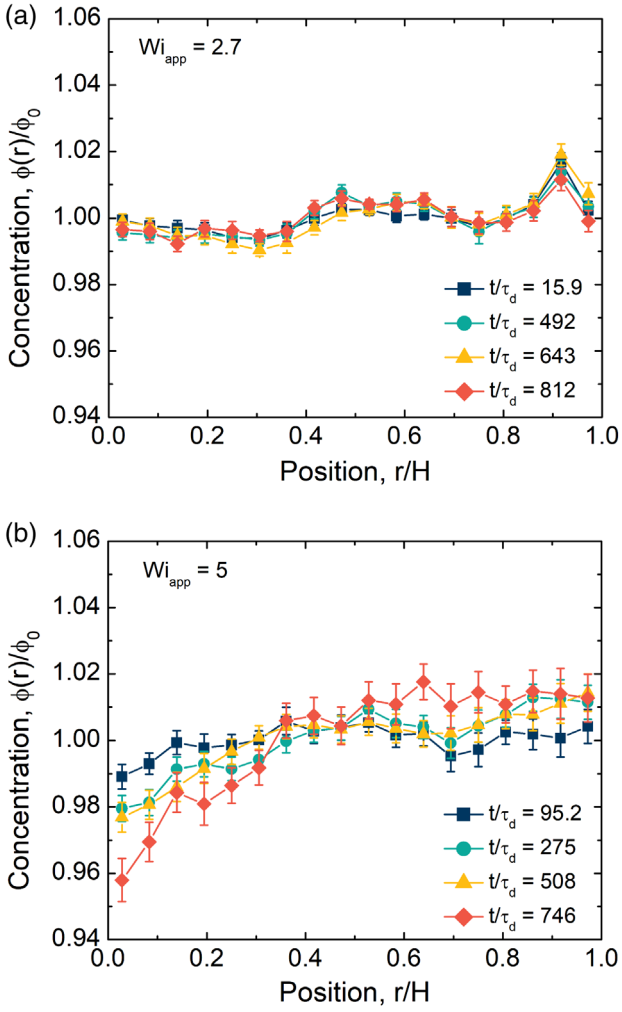

FIG. 4. Transient evolution of the concentration profile as measured from rheofluorescence under an applied shear flow of (a) $Wi_{app} = 2.7$ and (b) $Wi_{app} = 5$. Error bars represent the standard error associated with the fluorescence pixel intensities within each bin.

Fig. 4 for $Wi_{app} = 2.7$ and 5. For $Wi_{app} = 5$, significant nonuniformities develop over time, consistent with flow-concentration coupling. After shearing for $t/\tau_d = 95.2$, the concentration is depleted near the moving wall ($r/H = 0.0$) and enriched near the stationary wall ($r/H = 1.0$). The direction of this change in concentration across the fluid qualitatively agrees with the expectation that polymer migration occurs across curved streamlines in which the polymer moves to regions of lower shear stress [39,56,57]. A similar evolution of the concentration profiles occurs for all other cases considered $Wi_{app} = 3.25$, 6, and 8, with the exception of $Wi_{app} = 2.7$. For this case, the measured concentration profiles in Fig. 4(a) do not show appreciable change over the duration of steady shearing, with the normalized concentration remaining around 1.00.

The resulting measured estimates of the longtime concentration profiles from rheofluorescence were found to

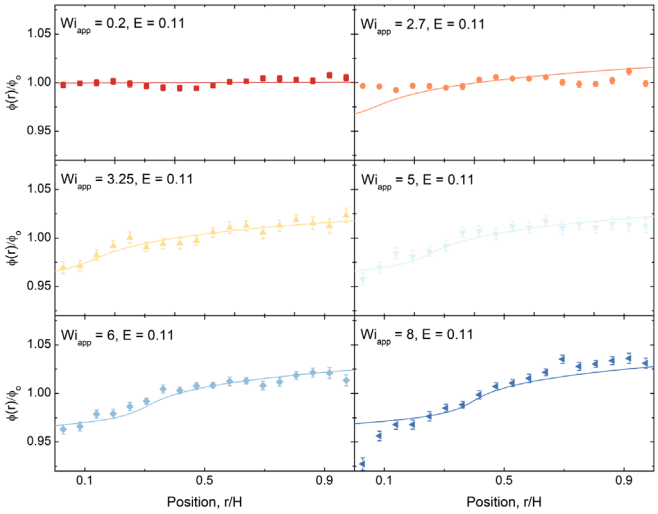

FIG. 5. Steady-state concentration profiles at varying Wi_{app}. Symbols reflect experimentally measured concentration estimates from rheofluorescence and solid lines correspond to model predictions for $E = 0.11$. Error bars represent the standard error associated with the fluorescence pixel intensities within each bin.

agree quantitatively with the two-fluid model predictions for $E = 0.11$ without any adjustable parameters (Fig. 5). As described earlier, this value of E was determined from best fits of the model predictions to the measured flow profiles using rheo-PTV, a totally independent measurement from rheofluorescence. An upper bound on the timescale for changes in concentration across the fluid is therefore estimated to be 1250 s based on the Einstein-Smoluchowski relation $D = H^2/2t$, where H is the fluid thickness (500 μm). Based on the scaling relation $D \sim M^{-2}$, where M is the polymer molecular weight, the polymer diffusivity is estimated to be $O(10^{-10}\ m^2/s)$.Thus, it is believed the fluorescence profiles reported in Fig. 5, which were taken at least 1400 s after the start of shear flow, represent the longtime concentration dynamics. These changes in the measured concentration profile are found to occur over longer timescales than what is required for the velocity profile to reach an apparent steady state. We believe the velocity profile banding initiates on short timescales following shear startup in the absence of changes to the concentration profile as discussed in detail by Adams *et al.* [58,59]. The two-fluid theory shows that the velocity profile evolves as a consequence of the changes in the concentration profile when the flow and fluid are initially homogeneous, but it is not clear in the current experiments whether the concentration nonuniformity drives the changes in the velocity profile or vice versa. Regardless of the transient evolution, with the exception of the case $Wi_{app} = 2.7$, both the magnitude of concentration change across the fluid and the interface location at steady state agree with the model predictions.

The measured concentration profile at $Wi_{app} = 2.7$ suggests that the fluid concentration remains uniform under

shear, though both the theory and the measured velocity profile indicate it should change. This apparent discrepancy likely results from the proximity of $Wi_{app} = 2.7$ to the stability boundary, where the two-fluid model predicts coexistence of both a banded and a nonbanded solution depending on the startup protocol [38]. The velocity and concentration profiles were obtained in two separate experiments with significantly different startup protocols as noted in the description of the flow devices. We speculate that the milder startup protocol in the concentration measurements compared to the velocity measurements bypasses instability [38]. The difference in startup protocol is not expected to change the final steady-state profiles for Wi_{app} values away from the stability boundary, consistent with our results at higher Wi_{app}.

Nevertheless, at higher Wi_{app}, the agreement in experimental flow and concentration measurements with the two-fluid model predictions is strong support for steady profiles involving a shear-induced demixing of polymer and solvent. The only other noticeable difference between the model and the measured concentration is the two data points nearest the inner wall for $Wi_{app} = 8$. We are uncertain why this discrepancy arises, but suspect that it could arise from uncertainty in the measurement near the boundary due to the continuously moving inner wall during the time period in which fluorescence is measured; however, we do not believe that it significantly alters the basic conclusion that quantitative agreement between experiment and model predictions is remarkable considering that the particular value of E used was determined completely independently from the rheofluorescence measurements.

This study reveals new physics regarding a mechanism for the existence of shear banded velocity profiles in entangled polymers. The rheofluorescence measurements confirm that nonhomogeneous velocity profiles appear concomitant with nonlocal flow-concentration coupling, a notion that, until now, was based on purely theoretical grounds. Additionally, these results present the first experimental evidence for banding in entangled polymer solutions that is corroborated by spatially resolved theoretical predictions. Transient emergence of macroscopic concentration nonuniformity is found to occur at high Wi_{app} and leads to banded concentration profiles that coincide with banded velocity profiles. Strong agreement between the measured velocimetry and concentration profile data with two-fluid model predictions for nonzero values of E suggests an importance of the constituent polymer chemistry on the observed flow behavior, beyond what is intrinsic to the rheological parameters. To investigate this hypothesis, a systematic study of varying polymer chemistry and/or solvent quality to understand the impact of these variables on the resulting value of E is needed. Differences in E between different polymer systems could explain the longstanding disagreement in the measured flow behavior of entangled polymer-solvent systems of different chemical composition.

We suspect that the observations made here will catalyze a number of new investigations into the coupling of changes in concentration to the microstructure and bulk flow behavior of entangled polymer systems. The physics of shear-induced demixing in polymer solutions is also relevant to entangled polymer blends, where essentially the same theory predicts that a force imbalance due to chains of different molecular weights leads to spatial nonuniformities in the molecular weight distribution, which could have similar consequences on the flow [60]. We further anticipate that this evidence for flow-concentration coupling will inspire *in situ* concentration measurements to become more commonplace in the complex fluids community, where modifications to this rheofluorescence technique can be made to isolate the dynamics of the different components within the fluid. Finally, and perhaps the most important outcome of this study, is the suggestion that theoretical studies of the non-Newtonian flow behavior of polymer solutions must account for the possibility of changes in the flow due to coupling between the polymer concentration and the stress.

M. C. B. and M. E. H. acknowledge support from the National Science Foundation under Grant No. CBET-1729108. L. G. L. acknowledges support from National Science Foundation under Grant No. CBET-1510333. C. M. B. acknowledges support from the National Science Foundation under Grant No. DMR-1844987. The authors thank Anton Paar for the opportunity to use the MCR 702 rheometer as part of the Anton Paar VIP program.

*Corresponding author.
lgleal@ucsb.edu
†Corresponding author.
helgeson@ucsb.edu

[1] M. Doi and S. F. Edwards, J. Chem. Soc., Faraday Trans. **74**, 1789 (1978).
[2] M. Doi and S. F. Edwards, J. Chem. Soc., Faraday Trans. **74**, 1802 (1978).
[3] G. Marrucci and N. Grizzuti, J. Rheol. **27**, 433 (1983).
[4] P. D. Olmsted, Rheol. Acta **47**, 283 (2008).
[5] T. Divoux, M. A. Fardin, S. Manneville, and S. Lerouge, Annu. Rev. Fluid Mech. **48**, 81 (2016).
[6] J.-B. Salmon, A. Colin, S. Manneville, and F. Molino, Phys. Rev. Lett. **90**, 228303 (2003).
[7] M. R. López-González, W. M. Holmes, P. T. Callaghan, and P. J. Photinos, Phys. Rev. Lett. **93**, 268302 (2004).
[8] M. W. Liberatore, F. Nettesheim, N. J. Wagner, and L. Porcar, Phys. Rev. E **73**, 020504 (2006).
[9] M. R. Lopez-Gonzalez, W. M. Holmes, and P. T. Callaghan, Soft Matter **2**, 855 (2006).
[10] M. E. Helgeson, P. A. Vasquez, E. W. Kaler, and N. J. Wagner, J. Rheol. **53**, 727 (2009).

[11] K. W. Feindel and P. T. Callaghan, Rheol. Acta **49**, 1003 (2010).
[12] J. F. Berret and Y. Séréro, Phys. Rev. Lett. **87**, 048303 (2001).
[13] S. A. Rogers, D. Vlassopoulos, and P. T. Callaghan, Phys. Rev. Lett. **100**, 128304 (2008).
[14] R. Besseling, L. Isa, P. Ballesta, G. Petekidis, M. E. Cates, and W. C. K. Poon, Phys. Rev. Lett. **105**, 268301 (2010).
[15] S. Ravindranath, S.-Q. Wang, M. Olechnowicz, and R. P. Quirk, Macromolecules **41**, 2663 (2008).
[16] Y. T. Hu, J. Rheol. **54**, 1307 (2010).
[17] P. E. Boukany, S.-Q. Wang, S. Ravindranath, and L. J. Lee, Soft Matter **11**, 8058 (2015).
[18] S. Jaradat, M. Harvey, and T. A. Waigh, Soft Matter **8**, 11677 (2012).
[19] K. A. Hayes, M. R. Buckley, I. Cohen, and L. A. Archer, Phys. Rev. Lett. **101**, 218301 (2008).
[20] K. A. Hayes, M. R. Buckley, H. Qi, I. Cohen, and L. A. Archer, Macromolecules **43**, 4412 (2010).
[21] Y. Li, M. Hu, G. B. McKenna, C. J. Dimitriou, G. H. McKinley, R. M. Mick, D. C. Venerus, and L. A. Archer, J. Rheol. **57**, 1411 (2013).
[22] S.-Q. Wang, G. Liu, S. Cheng, P. E. Boukany, Y. Wang, X. Li, Y. Li, M. Hu, G. B. McKenna, C. J. Dimitriou, G. H. McKinley, R. M. Mick, D. C. Venerus, and L. A. Archer, J. Rheol. **58**, 1059 (2014).
[23] Y. Li and G. B. McKenna, Rheol. Acta **54**, 771 (2015).
[24] Y. Li, M. Hu, G. B. McKenna, C. J. Dimitriou, G. H. McKinley, R. M. Mick, D. C. Venerus, and L. A. Archer, J. Rheol. **58**, 1071 (2014).
[25] S. Lerouge and P. D. Olmsted, Front. Phys. **7**, 1 (2020).
[26] Y. T. Hu, L. Wilen, A. Philips, and A. Lips, J. Rheol. **51**, 275 (2007).
[27] W. W. Graessley, Adv. Polym. Sci. **16**, 1 (1974).
[28] E. V. Menezes and W. W. Graessley, J. Polym. Sci. Part B Polym. Phys. **20**, 1817 (1982).
[29] D. W. Mead, R. G. Larson, and M. Doi, Macromolecules **31**, 7895 (1998).
[30] S. T. Milner, T. C. B. McLeish, and A. E. Likhtman, J. Rheol. **45**, 539 (2001).
[31] A. E. Likhtman and T. C. B. McLeish, Macromolecules **35**, 6332 (2002).
[32] R. S. Graham, A. E. Likhtman, T. C. B. McLeish, and S. T. Milner, J. Rheol. **47**, 1171 (2003).
[33] A. E. Likhtman and R. S. Graham, J. Nonnewton. Fluid Mech. **114**, 1 (2003).
[34] S.-Q. Wang, S. Ravindranath, and P. E. Boukany, Macromolecules **44**, 183 (2011).
[35] S. Shin, K. D. Dorfman, and X. Cheng, Phys. Rev. E **96**, 062503 (2017).
[36] E. J. Hemingway and S. M. Fielding, Phys. Rev. Lett. **120**, 138002 (2018).
[37] M. Cromer, M. C. Villet, G. H. Fredrickson, and L. G. Leal, Phys. Fluids **25**, 051703 (2013).
[38] M. Cromer, G. H. Fredrickson, and L. G. Leal, Phys. Fluids **26**, 063101 (2014).
[39] J. D. Peterson, M. Cromer, G. H. Fredrickson, and L. G. Leal, J. Rheol. **60**, 927 (2016).
[40] X. F. Yuan and L. Jupp, Europhys. Lett. **60**, 691 (2002).
[41] S. M. Fielding and P. D. Olmsted, Phys. Rev. E **68**, 036313 (2003).
[42] S. M. Fielding and P. D. Olmsted, Phys. Rev. Lett. **90**, 224501 (2003).
[43] S. M. Fielding and P. D. Olmsted, Eur. Phys. J. E **11**, 65 (2003).
[44] By "macroscopic length scales" we refer to length scales comparable to the flow domain (i.e., in shear flow, comparable to the gap width between the bounding surfaces).
[45] X. L. Wu, D. J. Pine, and P. K. Dixon, Phys. Rev. Lett. **66**, 2408 (1991).
[46] E. Helfand and G. H. Fredrickson, Phys. Rev. Lett. **62**, 2468 (1989).
[47] P. K. Dixon, D. J. Pine, and X. L. Wu, Phys. Rev. Lett. **68**, 2239 (1992).
[48] K. Migler, C. H. Liu, and D. J. Pine, Macromolecules **29**, 1422 (1996).
[49] J. W. van Egmond, D. E. Werner, and G. G. Fuller, J. Chem. Phys. **96**, 7742 (1992).
[50] T. Kume, T. Hashimoto, T. Takahashi, and G. G. Fuller, Macromolecules **30**, 7232 (1997).
[51] See Supplemental Material at http://link.aps.org/supplemental/10.1103/PhysRevLett.126.207801 for PBDC synthesis details, linear rheological data, two-fluid R-P model equations, additional model calculations, and a shear-induced demixing state diagram.
[52] Y. T. Hu and A. Lips, J. Rheol. **49**, 1001 (2005).
[53] P. Cheng, M. C. Burroughs, L. G. Leal, and M. E. Helgeson, Rheol. Acta **56**, 1007 (2017).
[54] M. C. Burroughs, A. M. Shetty, L. G. Leal, and M. E. Helgeson, Phys. Rev. Fluids **5**, 043301 (2020).
[55] E. Raspaud, D. Lairez, and M. Adam, Macromolecules **28**, 927 (1995).
[56] M. J. MacDonald and S. J. Muller, J. Rheol. **40**, 259 (1996).
[57] K. A. Dill and B. H. Zimm, Nucleic Acids Res. **7**, 735 (1979).
[58] J. M. Adams and P. D. Olmsted, Phys. Rev. Lett. **102**, 067801 (2009).
[59] J. M. Adams, S. M. Fielding, and P. D. Olmsted, J. Rheol. **55**, 1007 (2011).
[60] J. D. Peterson, G. H. Fredrickson, and L. G. Leal, J. Rheol. **64**, 1391 (2020).